# INVESTIGATION OF THE GROUND MOTION NEAR THE LEANING TOWER OF BAD FRANKENHAUSEN USING SENTINEL-1 PERSISTENT SCATTERER INTERFEROMETRY

Jannik Jänichen[1], Clémence Dubois[1], Marco Wolsza[1], Nesrin Salepci[1], Christiane Schmullius[1]

[1] Department for Earth Observation, Institute of Geography, Friedrich-Schiller University, Jena, Germany – (jannik.jaenichen, clemence.dubois, marco.wolsza, nesrin.salepci, c.schmullius)@uni-jena.de

**Commission III, WG III/3**

**KEY WORDS:** Persistent Scatterer Interferometry, infrastructure monitoring, time series, building deformation

**ABSTRACT:**

Persistent Scatterer Interferometry (PSI) is a well-established technique for monitoring millimetre deformation of the Earth's surface. The availability of free and open SAR data with a repeat cycle of 6-12 days from the Copernicus mission Sentinel-1, allows PSI to be used complementary to traditional surveying techniques. Whilst the data resolution may not allow a precise determination of the geolocation of the occurring deformation, observed deformation patterns can be analysed with auxiliary data and often show correlation with the location of geophysical processes or human activities. In this paper, we investigate the particular case of the church tower of Bad-Frankenhausen in the north of the Free State Thuringia, Germany, with PSI processing of Sentinel-1 data. Both pass directions (descending and ascending) are considered, and different motion models are tested in order to retrieve the most accurate displacement pattern around the church location. Deformation up to -6 mm/yr are observed near the church location for the period 2016-2019 in ascending direction.

## 1. INTRODUCTION

### 1.1 Motivation

In urban areas, observed ground motion is often the result of both geophysical and anthropogenic processes. Indeed, ground subsidence may occur due to a specific geophysical process but can be enforced by e.g. building load, often causing infrastructure stability problems. Whilst ground subsidence may affect large regions, it may also be confined to limited areas, strongly correlated with the underground structure. Advances in Differential SAR Interferometry in the last twenty years allow the dense characterisation of those deformations. Especially, Persistent Scatterer Interferometry (PSI - Ferretti et al., 2001) is a particularly well-suited method for detecting and estimating local deformation patterns in urban areas. One principal advantage lies in the dense spatial estimation of ground motion, with a few millimetres magnitude accuracy.
Furthermore, the availability of free and open SAR data with a repeat cycle of 6-12 days from the Copernicus mission Sentinel-1 since 2014, makes the regular monitoring of infrastructures with the PSI technique an essential tool for complementing traditional surveying techniques.
In this study, we examine the particular example of the leaning tower of Bad Frankenhausen, using the PSI technique with Sentinel-1 data. We identify Persistent Scatterer near the tower location and analyse their deformation in comparison with their surroundings in order to better delimitate the area of motion and characterize the particular deformation of this area.

### 1.2 State-of-the-Art

Infrastructure monitoring using PSI has been performed in many approaches already, e.g. for the monitoring of road and railway networks (Delgado Blasco et al., 2019; North et al., 2017), bridges (Sousa et al., 2013; Huang et al., 2018), dams (Milillo et al., 2016), or cultural heritage areas (Is et al., 2010; Solari et al., 2016). Among those approaches, buildings represent a large part of the existing monitoring applications, either to analyse building deformation due to thermal expansion (Gernhardt et al., 2010) or the possible impact of geophysical processes such as landslides on building stability (Tofani et al., 2013).

Usually built on different fundaments as their surroundings, such infrastructures often present particular deformation patterns in comparison to their direct neighbourhood. Approaches for the automatic detection of such irregular patterns in space and time have been developed already (Zhu et al., 2018), few also considering the interaction between geology and observed subsidence (Pratesi et el., 2016; North et al., 2017). While some approaches rely principally on the velocity estimates for clustering (Kalia, 2018; Aslan, 2020), other approaches consider the time series of the displacements for identifying different deformation regimes (Zhu et al., 2018). This information is particularly important for infrastructure analysis, as many factors may impact the deformation (e.g. foundation, building load, specific lithology at the infrastructure location).
In this work, we analyse such a local deformation pattern, and fit different deformation models in order to accurately estimate its deformation regime and the difference to its direct surroundings.

This paper is structured as follows. Section 2 shows an overview of the study area and its geological setting, and gives information about the data used for the analysis. Section 3 presents the applied methodology for PSI processing and phase model regression. The results of the analysis are shown in Section 4, and validated with data from an independent PSI processing. Finally, Section 5 discusses the results with regard to the accuracy of the different deformation models and the current situation of the deformation at the tower location.

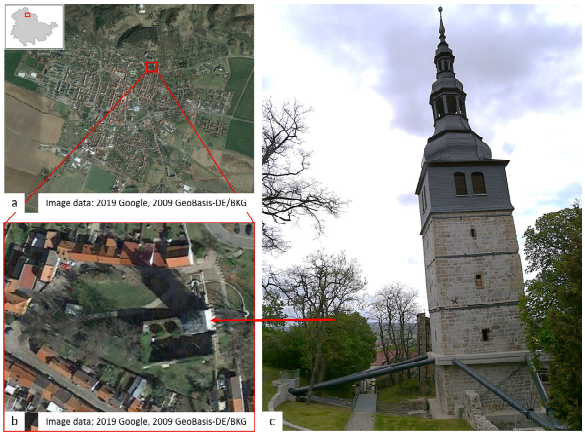


Figure 1: Overview of a) the city of Bad Frankenhausen; b) magnification of the image at the church location (Image data: 2019 Google, 2009 GeoBasis-DE/BKG); c) North view of the Church Tower

## 2. STUDY AREA AND DATA

### 2.1 Study area

Our study area is the city of Bad Frankenhausen, situated in the North of the Free State Thuringia (Germany) and at the southern border of the Kyffhäuser mountain range. This region throve in the last century through the mining of potash. Intensive mining in the late part of the century resulted in subsidence of whole cities situated over old mine shafts, leading to backfilling activities that have been monitored since using PSI (Dubois et al., 2020; Salepci, 2015).

The geological setting of the region of Bad Frankenhausen is characterized by soluble Permian sediments and various fault zones, like the West-East-trending Kyffhäuser Southern Margin Fault (KSM Fault). This particular geological setting results in a high susceptibility to subrosion processes and the occurrence of sinkholes in this region (Wadas, 2016). One consequence of the subsurface dissolution of material can be seen in the leaning church tower of Bad Frankenhausen, which today is a major tourist attraction. Around 1640 the church tower started to tilt towards the East (Kaufmann, 2019) and with a mean inclination of 4.9° it has been described as one of the most inclined historical towers of the world (Hallermann, 2015).

Research on the underlying geodynamic processes and subsequent measures to ensure the stability of this historical building have been carried out since decades (Findeisen, 1998). Recent studies show that the subsidence of the area surrounding the church tower is still ongoing. A precise levelling survey has been conducted since 1997/1999 by (Scheffler et al., 2013) and reveals irregular, but also decreasing movement rates of the church tower (~8 cm/yr between 2003-2005 and 3,5 cm/yr between 2010-2012). Furthermore, a high-precision time-lapse gravity and levelling survey was published by Kobe et al. (2019), which also shows continuous subsidence in our study area due to subrosion-induced mass changes.

To our current knowledge, no specific analysis of this subsidence process has been performed using SAR Interferometry yet, which makes this study even more interesting for complementing the gravity and levelling surveys.

| Dataset | Direction of acquisition | Relative orbit number | Number of acquisitions | Timespan of the acquisitions |
|---|---|---|---|---|
| 1 | Ascending | 117 | 191 | 13/10/2014 – 15/01/2020 |
| | | | Reduced to 44 | 11/05/2016 – 10/12/2019 |
| 2 | Descending | 66 | 55 | 10/10/2014 – 11/04/2019 |

Table 1: Sentinel-1 datasets and acquisition parameters

### 2.2 Data

In this study, we use two different datasets of the Copernicus mission Sentinel-1, which acquisition parameters are listed in Table 1. We considered both directions of acquisition (ascending and descending) separately. The church tower is surrounded by trees in the East and ruins of the ancient church walls in the South-West (see Figure 1b and 1c). For the descending setting, trees may hamper the signal to reach the tower. As for the ascending setting, the building walls are also hidden in the West with trees but may produce an additional backscatter in the open areas (Figure 1b). However, as the tower is higher than the ruins or the trees, a backscatter coming from multiple bounces within the belfry structure, in either direction, can be expected. Furthermore, as the tower is tilting to the East, a combination of ascending and descending deformation is interesting to retrieve the East-West deformation instead of the sole Line-of-Sight (LOS) deformation component available for a single acquisition direction. For both acquisition directions, we considered data from the start of the Sentinel-1 mission up to recent months, in order to have a 5-year deformation estimate. However, non-resolved processing problems during the analysis of the ascending dataset constrained us to consider only data from 2016 to 2019 for now (the data marked in grey in Table 1 correspond to the original dataset and the black ones correspond to the refined dataset). In order to reduce processing time whilst keeping the possibility for regular monitoring, we considered for both acquisitions directions only data from Sentinel-1A and reduced the data rate at one acquisition per month. This leads to a total number of 55 acquisitions between 10/10/2014 and 11/04/2019 for the descending, and of 44 acquisitions between 11/05/2016 and 10/12/2019 for the ascending orbit.

For the PSI processing, several external datasets have been used. For the selection of a suitable master scene, weather data from the German Meteorological Service at the weather station Artern, situated 13km east of Bad Frankenhausen, has been used. Here we considered information about relative and absolute humidity, atmospheric pressure, precipitation and air temperature in order to identify a master scene where the phase delay through the atmosphere can be assumed to be low. Furthermore, a 5 m resolution LIDAR DEM was available and used for different steps of the processing (coregistration, calculation of the differential interferograms and geocoding). This DEM was provided by the Thuringian Institute for Environment, Mining and Nature Conservation.

For the validation of the results, no ground motion information (e.g. levelling information) was available except the one found in the literature. However, we used an independent PSI dataset produced in the framework of the German Ground Motion Service (BGR 2019). This service provides mean velocity and corresponding displacement time series for Persistent Scatterer

(PS) detected in the ascending direction between 2014 and 2018. While a direct comparison to our data is not possible due to the different period of observations and partially different acquisition direction, this dataset allows a coarse cross validation of our observation for the period 2014 - 2018, as the observed motion patterns should be similar.

## 3. METHODOLOGY

In this work, we performed PSI processing of both acquisition directions (ascending and descending) separately. Afterwards, we analysed the possibility of combining both results for an accurate estimation of the East-West motion of the church tower. The PSI analysis is performed using the IPTA (Interferometric Point Target Analysis) module of the GAMMA Remote Sensing software version 1.8 and is based on the PSI method presented in (Ferretti, 2001).

An optimal master scene was selected by considering the temporal and perpendicular baseline, as well as weather conditions in order to prevent the influence of atmospheric disturbances as much as possible. For the coregistration of all slave scenes with the master scene, a high-resolution LIDAR DEM was used, which decreased possible errors due to offsets in the topography. PS candidates were then selected using two different approaches. First, the Amplitude Dispersion Index (ADI) developed by Ferretti et al. (2000, 2001), which is based on the temporal variability of the backscatter coefficient was used. Second, the Spectral Phase Diversity (SPD) was used, which indicates the variation of the phase power spectrum. Scatterer showing both low ADI and low SPD were retained as potential PS candidates. Subsequently the differential interferograms are calculated and a two-dimensional regression analysis is performed on the phase values, while considering spatial and temporal phase differences.

In general, the deformation component of the phase can be modelled for an arc between PS candidate $i$ and $j$ according to van Leijen, (2014), as follows:

$$\varphi_{i,j} = \sum_{p=1}^{P} a_p(B_T) D_p \tag{1}$$

$P$ represents the number of models, $a_p$ describes a deformation model with deformation parameters $D_p$, as function of the vector $B_T$ of temporal baselines.

A simple linear model would be written as

$$a_1 = -\frac{4\pi}{\lambda} B_T \tag{2}$$

where the wavelength $\lambda$ and the temporal baseline $B_T$ determine the maximum deformation rate measurable (van Leijen, 2014). Based on Eq. (1), more complex deformation models can be applied, e.g. through the use of breakpoints characterizing a change of deformation regimes or the use of higher-order polynomial allowing the retrieval of non-linear deformations such as acceleration or deceleration of the deformation rate (van Leijen, 2014).

In this work, we considered seven different phase models available in the GAMMA Software. Those seven models are summarized in Table 2 with our interpretation. More information can be found in Werner et al., (2003). The notations correspond to the one found in the GAMMA software whereby *delta_t* correspond to the previously defined $B_T$ and *aX* correspond to $D_p$. The parameter *bperp* corresponds to the geometrical perpendicular baseline.

| # | Phase model | Signification |
|---|---|---|
| 1 | a0 | Constant phase |
| 2 | a1 * bperp | Phase is only dependent on the perpendicular baseline, the slope of the regression indicates the relative height correction. Information about the deformation phase is provided together with the atmospheric and noise component. |
| 3 | a2 * delta_t | Linear phase dependency with time, constant deformation rate equivalent to Eq.(2) |
| 4 | a1 * bperp + a2 * delta_t | Phase is dependent of both perpendicular baseline (height correction) and time. Constant deformation rate. |
| 5 | a0 + a1 * bperp + a2 * delta_t | Sum of all models, can assume a constant phase offset, estimates precise relative height correction and linear deformation depending on the temporal baseline |
| 6 | a0 + a2 * delta_t | Sum of model 1 and 3, height estimation might not be exact |
| 7 | a0 + a1 * bperp | Sum of model 1 and 2, no possibility to distinguish the deformation from the atmospheric component |

Table 2: Different phase models considered in this work (after Werner et al., 2003).

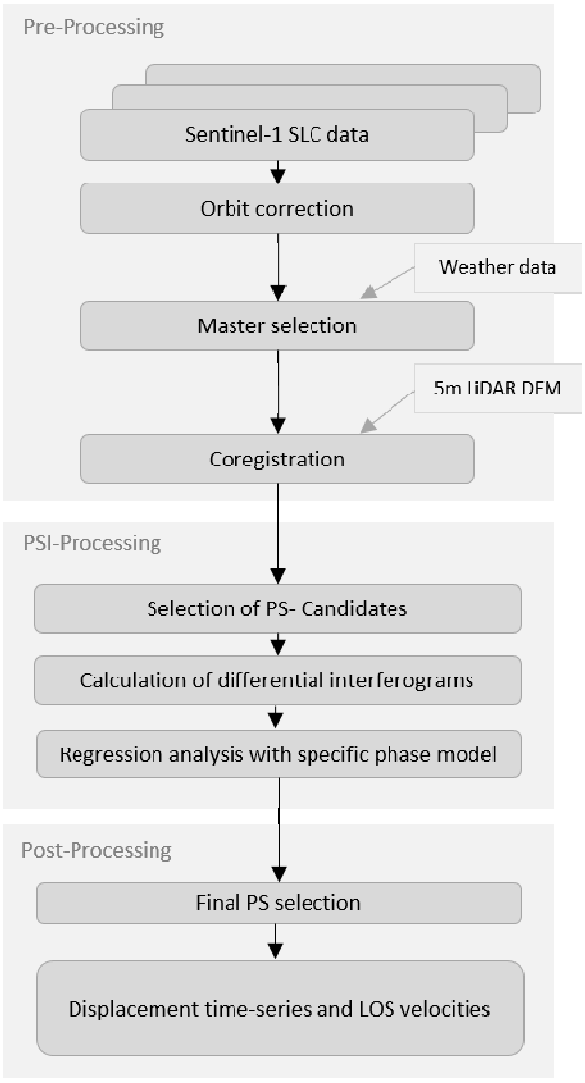


Figure 2: Workflow of the methodology

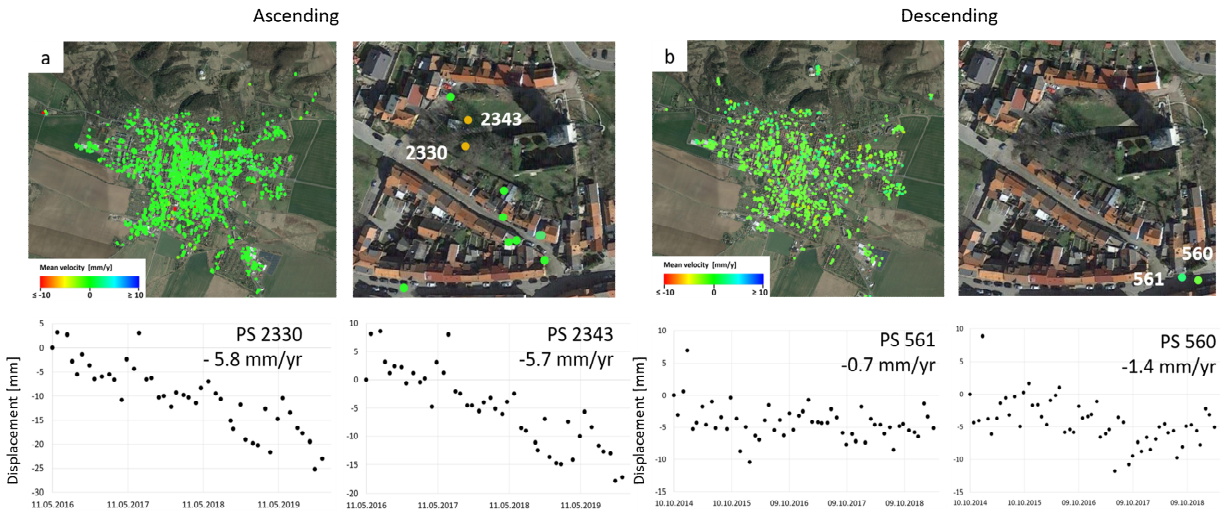


Figure 3: Velocity maps of Bad Frankenhausen for a) ascending (2016-2019) und b) descending (2014-2019) directions

For the regression analysis, a reference point was chosen in a stable area, where its displacement rate is assumed negligible over time. Therefore, the calculated relative displacements to this point may be considered as absolute deformations.
Figure 2 shows the overall workflow of our methodology, to be considered individually for both acquisition directions.

## 4. RESULTS

In this section, we present the results of the PSI analysis for both acquisition directions. Furthermore, we present time-series displacements of detected PSs situated close to the church tower and analyse their different profiles both visually and numerically in order to determinate which phase models are best suited for this area. Finally, we validate our results with data from the German Ground Motion Service.

### 4.1 Velocity maps

Figure 3 shows for both acquisition directions the resulting velocity maps of the selected PSs. Both maps show that the city area of Bad Frankenhausen is very stable, with estimated motion close to 0 mm/yr (green PSs) on most areas. Zooming in the area of interest, near the church tower, few PSs show higher velocity rates, indicating subsidence between -1 mm/yr (descending; Figure 3b) and -6 mm/yr (ascending; orange PSs in Figure 3a). It is visible, that no PS seem to be detected directly at the church location. However, few PSs are detected very near the church tower location, principally on adjacent infrastructures, for the ascending direction.
As the detected PSs in ascending and descending direction are situated on different structures, we analyse both directions separately and do not combine the results in order to estimated East-West motion.
For the descending direction, we analysed the two closest PSs to the tower (see Figure 3b). Those PSs are situated in the south east of the church on building or road infrastructure and register subsidence rates of -0.7 mm/yr and -1.4 mm/yr, respectively. They do not show a strong difference compared to the surrounding PSs and are therefore considered as stable. Their displacement profile (Figure 3b) show few irregularities that can be due to seasonal motion, and PS 560 seems more stable since the end of 2017.
For the ascending direction, two PSs could be identified recording higher subsidence as their surroundings: -5.7 mm/yr and -5.8 mm/yr, for PS 2343 and 2330 respectively (Figure 3a). Those PSs are situated in the West of the church on specific structures within the park surrounding the church (information kiosk and panel). As the detected PSs for the ascending direction are closer to the Church Tower and show higher deformation rate, we focus in the following on different deformation models for the ascending direction, focusing of the PSs situated closer to the church tower.

### 4.2 Displacements

Figure 4 shows for the selected PSs close to the church tower the displacement time series estimated using the seven different phase models presented in Table 2, for the ascending direction. Table 3 shows for each model the total number of detected PS, the estimated deformation rate, the standard deviation of the residual phase, the estimated height uncertainty and the estimated uncertainty on the deformation rate at the particular PS encircled in red in Figure 4.
It is observable that phase models 1, 2 and 7 show for all detected PSs a deformation rate of 0 mm/yr (Table 3 and Figure 4, left column). This is due to the phase model that does not take into account the linear dependency of the phase over time. A PS detected in the three models and situated in the South of the Church Tower has been analysed in more detail (Table 3 and Figure 4, right column). The displacement time series show little deformation over time, ranging from approx. -5 to +5 mm (Figure 4, right column). The height of the PS and the estimated height uncertainty are consistent for all three models. Those model show the highest standard deviation of the residual phase, with approximately 0.9 rad.
The remaining models (3, 4, 5 and 6) all consider linear phase dependency with time (Table 2), leading to the detection of linear subsidence near the church tower location. For each model, one to four PSs showing subsidence of -5.8 to -6.4 mm/yr have been detected (Table 3 and Figure 4, middle column). The deformation profiles (Figure 4, right column) show displacements up to approx. - 30 mm for the whole period of observation. For all models, a seasonal deformation seems to occur, with an uplift towards the sensor direction starting in spring every year, and increased subsidence during winter. As we consider deformation in the LOS direction, this could correspond to an increased

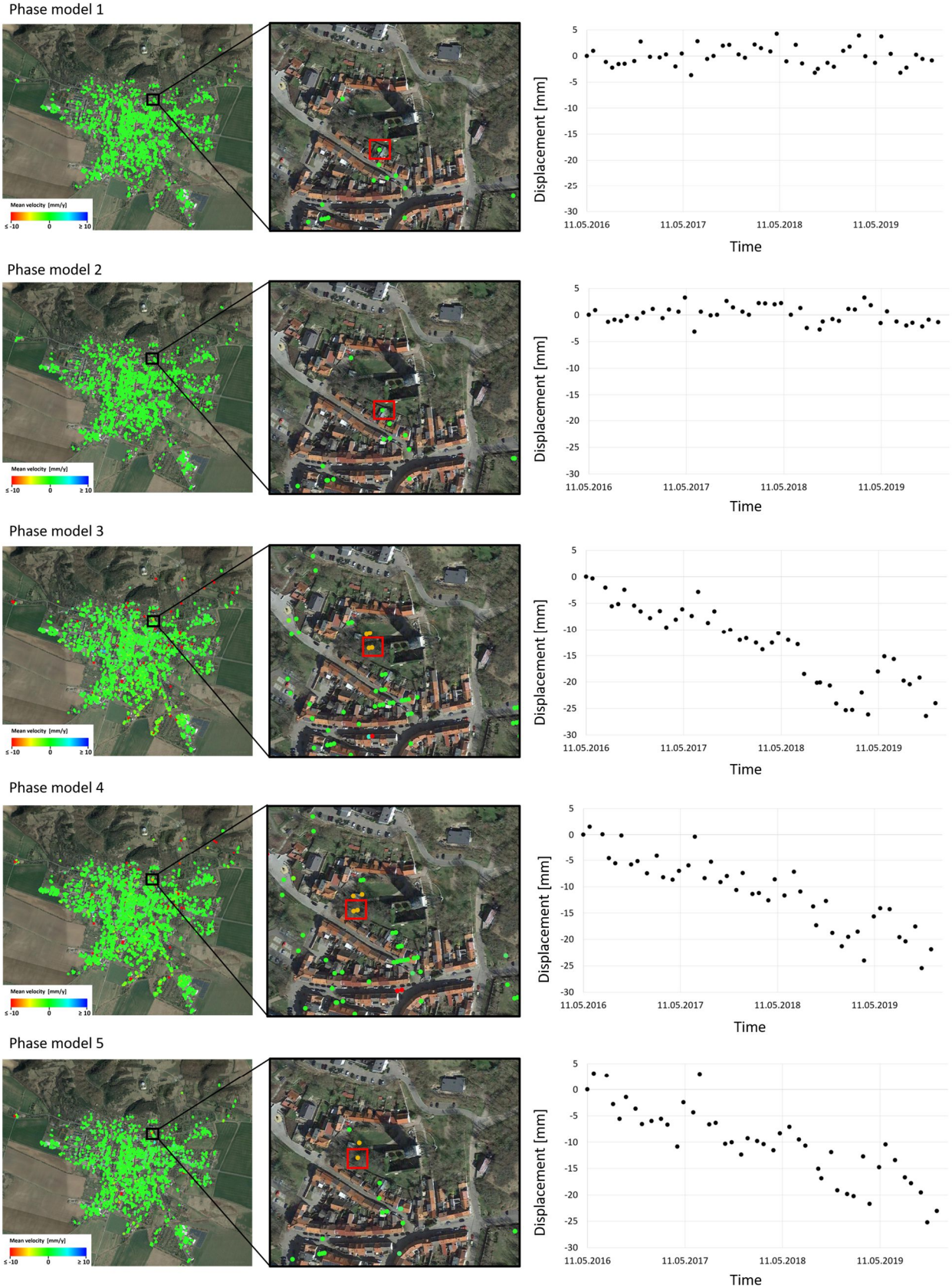


Figure 4: Time-Series displacements at the location of the Church Tower with different phase models; left: velocity map for the city of Bad Frankenhausen; middle: zoom-in to the church location; right: displacement profiles

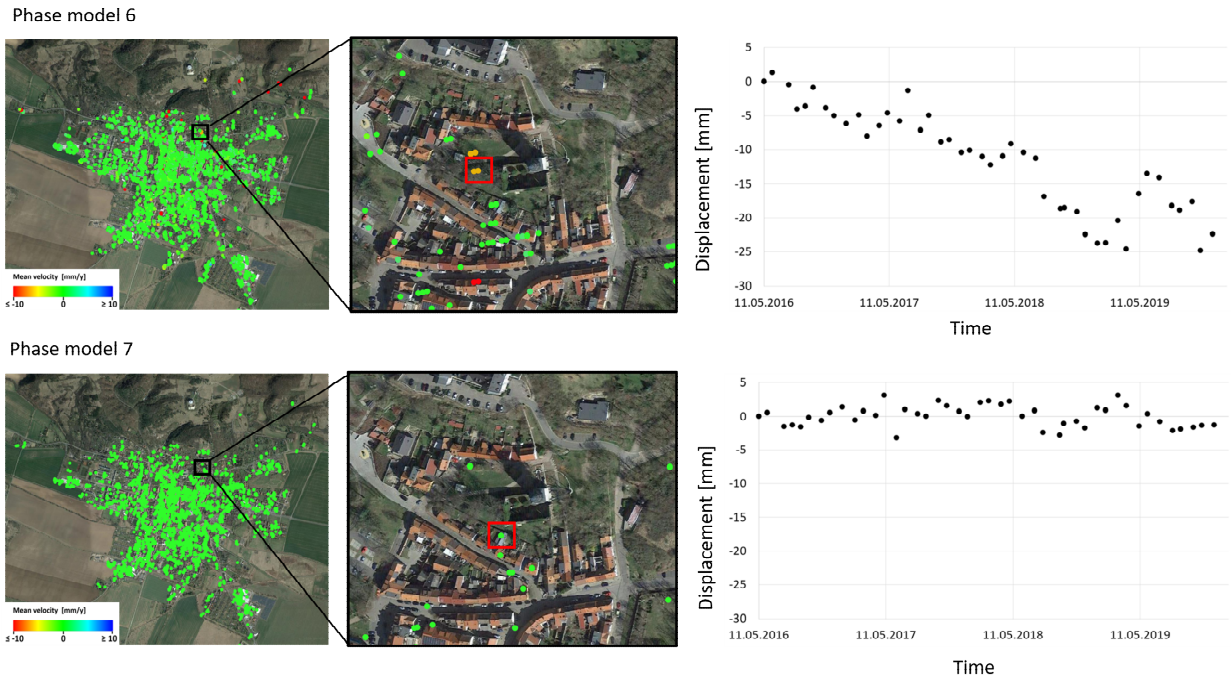


Figure 4bis: Time-Series displacements at the location of the Church Tower with different phase models; left: velocity map for the city of Bad Frankenhausen; middle: zoom-in to the church location; right: displacement profiles

leaning of the tower in the winter. This seasonal behaviour seems opposite for the other three phase models and would need further investigation considering meteorological and soil data. Table 3 indicates for model 5 a higher uncertainty of the estimated height value for the selected PS. Moreover, for models 3, 4 and 6 almost twice as many PSs were detected as for the other models (4300 against approx. 2500). A look at the disparity maps however shows for those models a stronger occurrence of single PSs with strong deformation compared to their surroundings (red dots in Figure 4, left column). A comparison between these three models and model 5 indicates a larger standard deviation of the residual phase, of 0.9 rad for the three models against 0.8 rad for model 5. This is also observed for the average of the dataset (not shown here). Because model 5 provides the less "noisy" velocity map while taking into account linear phase dependency and because it shows the smaller standard deviation of the phase residuals, we consider this model as best suitable for the following analysis.

### 4.3 Validation

As mentioned in Section 2.2., no in-situ data was available to validate our results. We therefore performed a coarse cross comparison of our velocity map using the products of the German Ground Motion Service (BGR 2019). Figure 5a shows the velocity maps resulting of our approach for the period 2016-2019 and Figure 5b shows the corresponding area from the German Ground Motion Service (GGMS) for the period 2014-2018. Both show velocity estimates from the ascending direction, the GGMS considered all available Sentinel-1A and -1B data, leading to an increase of the number of considered acquisitions starting for this region in March 2017. This is visible in Figure 5c where the time series displacements of the PS closest to the church tower

| Phase model | Number of detected PS | Deformation rate [mm/yr] | Estimated deformation rate uncertainty [mm/yr] | Height [m] | Estimated height uncertainty [m] | Standard deviation of the residual phase [rad] |
|---|---|---|---|---|---|---|
| 1 | 2510 | 0 | 0 | 152.2 | 0 | 0.9 |
| 2 | 2346 | 0 | 0 | 154.6 | 2.0 | 0.9 |
| 3 | 4300 | -5.8 | 0.6 | 151.1 | 0 | 0.8 |
| 4 | 4300 | -5.6 | 0.5 | 140.7 | 3.8 | 0.8 |
| 5 | 2618 | -5.8 | 0.5 | 146.6 | 6.2 | 0.7 |
| 6 | 4300 | -6.4 | 0.5 | 151.1 | 0 | 0.8 |
| 7 | 2538 | 0 | 0 | 154.5 | 3.0 | 0.9 |

Table 3: Estimated parameters for each model at the specific location of Figure 4 (red square)

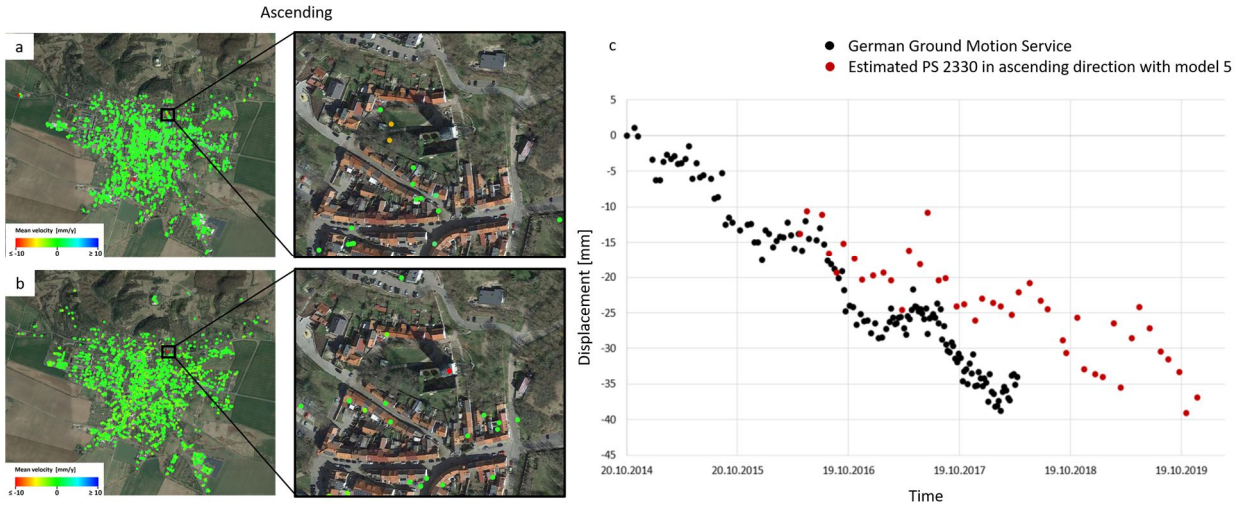


Figure 5: Comparison with auxiliary data a) proposed approach with phase model number 5; b) PSI from the German Ground Motion Service; c) comparison of extracted PSs near the Church Tower.

location in each dataset are represented. The black dots correspond to the PS situated at the church location in the dataset of the GGMS, the red dots correspond to the PS 2330 of Figure 3a.

The velocity maps show overall the same, stable pattern over the city area, which provides a coarse validation of our results. Considering the detected single PSs, the results differ. The PS found at the church tower location in the GGMS is not found in our approach, and the PSs of our approach do not appear in the GGMS. This could have different explanation. First, the periods considered are different for both datasets. Changes that happened on the church tower between April 2018 (end of the GGMS dataset) and December 2019 (end of our dataset) may have an influence on the detected scatterers. Second, the dataset from the GGMS not only uses both Sentinel-1A and Sentinel-AB data, leading to a very large dataset, but further investigation have shown that the orbit used was different. While our dataset is from relative orbit 117, the displacement time series of the detected PS in the GGMS dataset correspond to acquisition dates of relative orbit 44, situated eastward of orbit 117. Finally, the phase models used in both approaches may differ.

Even if the displacement profiles represented in Figure 5c do not represent the same PS in reality, a good correlation exists, as they both show a continuous subsidence since 2014 and 2016, respectively. According to the registered displacement rates, PS 2330 shows less deformation since 2016 than the PS detected in the GGMS.

## 5. DISCUSSION

The proposed approach allowed the detection of local motion patterns near the church tower location of Bad Frankenhausen for four specific phase models out of seven. All model considering linear phase dependency in function of the temporal baseline showed good results. The most complete model (model 5) considers constant phase offset, precise relative height correction and linear deformation depending on the temporal baseline and shows the lowest standard deviation of the residual phase of all models.

For our study, the ascending direction proved to be the better configuration for detecting deformation near the church location. It shows also good consistency with the data from the GGMS that we used to validate coarsely our results. Even if different PSs were detected in both datasets, the overall deformation rates in the city and close to the church location are consistent. Assuming the geolocation accurate for both approaches, the different deformation rates found in both approaches could be due to a different load on the surface, as the GGMS detected a PS directly at the tower location, which shows higher load as the metallic structure and small information point situated in the park nearby and detected in our approach.

In our approach, no PS could be detected directly on the church tower. This could have several reasons. First, the church tower underwent several restorations in the last five years. From Mai to November 2015, the church tower has been completely stabilized in order to reduce the mechanical deflection: the foundation has been renewed, a steel rim has been attached around the tower and steel pipes have been fixed on it and installed on two faces of the tower walls, in order to support the leaning construction (Figure 1c). This conservation work produces a lot of non permanent scatterer (trucks, fences, scaffolds and other moving objects) within a short perimeter that could hinder the detection of Permanent Scatterers. Beside remaining processing problems, this could explain why we did not get any reliable information using the ascending datastack from 2014 to 2020. An interesting observation is the detected PS at the church location in the dataset of the GGMS, which did not suffer from the construction yard. It is possible that this scatterer is situated high on the church structure and did not disappear throughout construction. The displacement profile however does not show a particular change of the displacement regime since the consolidation of the foundation, contrary to the expectations. Furthermore, a second change occurs near the church in 2018. During this year, the church spire has been replaced, leading to the construction of the temporary scaffolding around the tower (TH24, 2018), which can influence the backscatter at this location.

The second reason why we could not detect any PS directly at the church location could be the local conditions in combination with the acquisition configurations. Indeed, the church is situated in a park and surrounded on most sides by trees. In the considered ascending configuration, the church is situated between the middle and far range, leading to a rather flat incidence angle of 37°. The use of data from the neighbor orbit path would lead to a steeper incidence of approx. 29° and therefore allow different signal path and the possible detection of different PS at the church location.

## 6. CONCLUSION AND OUTLOOK

In this paper, we analysed the deformation of the city of Bad Frankenhausen using PSI. Particularly, we investigated very local deformation pattern at the location of a leaning church tower, and fit different deformation models in order to estimate the specific deformation regime at this location. A model taking into account both perpendicular baseline for height correction and temporal baseline to estimate the deformation provided the best results. Further investigation should focus on the use of other, non-linear models, allowing for the identification of different deformation regimes within a time series (e.g. breakpoints). Finally, data from the neighbouring orbit path should be investigated for this case.

## REFERENCES

Aslan, G., Foumelis, M., Raucoules, D., De Michele, M., Bernardie, S., & Cakir, Z., 2020. Landslide Mapping and Monitoring Using Persistent Scatterer Interferometry (PSI) Technique in the French Alps. *Remote Sensing*, 12(8), 1305.

BGR 2019 - BodenBewegungsdienst Deutschland (BBD) https://bodenbewegungsdienst.bgr.de/mapapps/resources/apps/bbd/index.html?lang=de (last access: 29.01.2020)

Delgado Blasco, J. M., Foumelis, M., Stewart, C., Hooper, A., 2019. Measuring Urban Subsidence in the Rome Metropolitan Area (Italy) with Sentinel-1 SNAP-StaMPS Persistent Scatterer Interferometry. *Remote Sensing*, 11(2), 129.

Dubois, C., Jänichen, J., Wolsza, M., Salepci, N., & Schmullius, C., 2020. 20 Years SAR Interferometry for Monitoring Ground Deformation over the former Potash-Mine "Glückauf" in Thuringia, *Tagungsband Geomonitoring 2020*, S. 29-45. DOI: https://doi.org/10.15488/9339.

Findeisen, C., Michalik, I., Schleußner, H. P., Slowik, V., 1998. Sanierungsvorschlag für den Turm der Oberkirche in Bad Frankenhausen/A proposal for the restoration of an inclining church tower at Bad Frankenhausen. *Restoration of Buildings and Monuments*, 4(4), 357-376.

Ferretti, A., Prati, C., Rocca, F., 2001. Permanent scatterers in SAR interferometry. *IEEE Transactions on geoscience and remote sensing*, 39(1), 8-20.

Gernhardt, S., Adam, N., Eineder, M., Bamler, R., 2010. Potential of very high resolution SAR for persistent scatterer interferometry in urban areas. *Annals of GIS*, 16(2), 103-111.

Hallermann, N., Morgenthal, G., Rodehorst, V., 2015. Vision-based monitoring of heritage monuments: Unmanned Aerial Systems (UAS) for detailed inspection and high-accuracy survey of structures. *WIT Transactions on The Built Environment*, 153, 621-632.

Huang, Q., Monserrat, O., Crosetto, M., Crippa, B., Wang, Y., Jiang, J., Ding, Y., 2018. Displacement monitoring and health evaluation of two bridges using Sentinel-1 SAR images. *Remote Sensing*, 10(11), 1714.

Is, P., Foumelis, M., Pavlopoulos, K., Kourkouli, P., 2010. Ground deformation monitoring in cultural heritage areas by time series SAR interferometry: The case of ancient Olympia site (Western Greece). *In Proceedings of the ESA FRINGE Workshop, Frascati, Italy* (Vol. 30).

Kaufmann, G., Romanov, D., 2019. Modelling speleogenesis in soluble rocks: A case study from the Permian Zechstein sequences exposed along the southern Harz mountains and the Kyffhäuser Hills, Germany. *Acta carsologica*, 48.

Kalia, A. C., 2018. Classification of landslide activity on a regional scale using persistent scatterer interferometry at the moselle valley (Germany). Remote Sensing, 10(12), 1880.

Kobe, M., Gabriel, G., Weise, A., Vogel, D., 2019. Time-lapse gravity and levelling surveys reveal mass loss and ongoing subsidence in the urban subrosion-prone area of Bad Frankenhausen, Germany. *Solid Earth*, 10(3), 599-619.

Milillo, P., Perissin, D., Salzer, J. T., Lundgren, P., Lacava, G., Milillo, G., Serio, C., 2016. Monitoring dam structural health from space: Insights from novel InSAR techniques and multi-parametric modeling applied to the Pertusillo dam Basilicata, Italy. *International journal of applied earth observation and geoinformation*, 52, 221-229.

North, M., Farewell, T., Hallett, S., Bertelle, A., 2017. Monitoring the response of roads and railways to seasonal soil movement with Persistent Scatterers Interferometry over six UK sites. *Remote Sensing*, 9(9), 922.

Pratesi, F., Tapete, D., Del Ventisette, C., Moretti, S., 2016. Mapping interactions between geology, subsurface resource exploitation and urban development in transforming cities using InSAR Persistent Scatterers: Two decades of change in Florence, Italy. *Applied Geography*, 77, 20-37.

Salepci, N. (2015). Multi-sensor synergy for persistent scatterer interferometry based ground subsidence monitoring (Doctoral dissertation).

Scheffler, T., Martienßen, T., 2013. Überwachungsmessungen zur Bestimmung der Deformationen von Kirchtürmen. Schriftenreihe des Instituts für Markscheidewesen und Geodäsie der TU Bergakademie Freiberg, 1, 83-96.

Solari, L., Ciampalini, A., Raspini, F., Bianchini, S., Moretti, S., 2016. PSInSAR analysis in the Pisa Urban Area (Italy): a case study of subsidence related to stratigraphical factors and urbanization. *Remote Sensing*, 8(2), 120.

Sousa, J. J., Bastos, L., Monserrat, O., Perski, Z., 2013. Multi-temporal SAR interferometry reveals acceleration of bridge sinking before collapse. *Natural Hazards & Earth System Sciences*, 13(3).

TH24, 2018.
https://www.thueringen24.de/thueringen/article215105035/Schiefer-Turm-von-Bad-Frankenhausen-verliert-seine-Krone.html, last access 24.04.2020.

Tofani, V., Raspini, F., Catani, F., Casagli, N., 2013. Persistent Scatterer Interferometry (PSI) technique for landslide characterization and monitoring. *Remote Sensing*, 5(3), 1045-1065.

Van Leijen, F. J., 2014. Persistent scatterer interferometry based on geodetic estimation theory (Doctoral Dissertation).

Wadas, S. H., Polom, U., Krawczyk, C. M., 2016. High-resolution shear-wave seismic reflection as a tool to image near-surface subrosion structures-a case study in Bad Frankenhausen, Germany. *Solid Earth*, 7(5), 1491.

Werner, C., Wegmuller, U., Strozzi, T., & Wiesmann, A., 2003. Interferometric point target analysis for deformation mapping. In IGARSS 2003. 2003 IEEE International Geoscience and Remote Sensing Symposium. Proceedings (IEEE Cat. No. 03CH37477) (Vol. 7, pp. 4362-4364). IEEE.

Zhu, M., Wan, X., Fei, B., Qiao, Z., Ge, C., Minati, F., Vecchioli, F., Li, J. & Costantini, M., 2018. Detection of building and infrastructure instabilities by automatic spatiotemporal analysis of satellite SAR interferometry measurements. *Remote Sensing*, 10(11), 1816.